BioMedical Engineering OnLine

RESEARCH

Open Access

Investigation of bending angle algorithm and path planning for puncture needles in transjugular intrahepatic portosystemic shunt

Qinmei Liao[1†], Bing Li[2†], Xihao Hu[1], Xiaoyun Huang[1], Jiacheng Guo[1], Yuanzhong Zhu[1] and Wenjing He[1*]

†Qinmei Liao and Bing Li have contributed equally to this work.

*Correspondence: hwj@nsmc.edu.cn

[1] School of Medical Imaging, North Sichuan Medical College, Nanchong 637000, China
[2] Department of Interventional Radiology, Affiliated Hospital of North Sichuan Medical College, Nanchong 637002, China

Abstract

Purpose: Design an algorithm to calculate the bending angle of the puncture needle for transjugular intrahepatic portosystemic shunt (TIPS) procedures and achieve three-dimensional visualized path planning.

Materials and methods: Based on enhanced CT images, a thresholding segmentation method was used to perform three-dimensional reconstruction of the hepatic vasculature, with the target puncture point selected by the interventional physician. The puncture needle was modeled using second-order Bézier curves and arcs. Subsequently, the bending points were selected, and the optimal bending angles were calculated based on the target puncture point. The puncture pathway was then verified and visualized in three dimensions using Mimics software. Data from 32 patients who successfully underwent TIPS procedures were retrospectively collected for clinical validation and statistical analysis.

Results: The error between the tip position of the puncture needle catheter modeled with Bézier curves and the actual puncture needle was 0.15 cm, while the error for the arc modeling was 0.19 cm. The optimal bending angle of the puncture needle calculated by this algorithm was validated in Mimics software, successfully achieving path planning. Among the 32 patients, the difference between the actual bending angle of the puncture needle and the calculated bending angle was $1.06° \pm 1.82°$ (95% CI 0.41–1.72°). The equivalence test results indicated that there was a significant equivalence between the measured angle and the angle calculated by the algorithm ($p < 0.001$).

Conclusion: This study successfully designed an algorithm for calculating the bending angle of the puncture needle in TIPS procedures, which demonstrated equivalence with the clinically observed bending angles.

Keywords: Bending angle, Path planning, Bézier curve, TIPS, Puncture needle

Introduction

Transjugular intrahepatic portosystemic shunt (TIPS) is a commonly used and effective method for treating complications of portal hypertension [1–3], such as refractory ascites [4] and esophageal–gastric variceal bleeding [5, 6]. Among the various steps in

the TIPS, the puncture from the hepatic vein to the portal vein is the most critical and challenging [7, 8]. The puncture kits commonly used in TIPS, such as the RUPS-100, feature a fixed bending angle at the front end of the puncture needle. However, due to the variations in the spatial positioning of the hepatic and portal veins in different patients, the puncture needle may not be suitable for personalized treatment. Currently, adjustments to the bending angle of the puncture needle primarily rely on the physician's experience, and inappropriate angle selection can lead to increased puncture attempts and extended surgical duration. Research has demonstrated that the correct selection of the bending angle and puncture distance of the needle is essential for accurately accessing the portal vein [9]. Research on the quantitative calculation of the bending angle of puncture needles is limited. Zhu et al. [10] conducted a study to quantify the bending angle of puncture needles; however, the designed bending region of the needle was only from the hepatic vein to the portal vein, which does not accurately reflect real-world conditions. Therefore, this study aims to quantitatively calculate the bending angle of the TIPS puncture needle based on CT images and to complete three-dimensional visualization for path planning, thereby laying the foundation for improving the accuracy of portal vein puncture in TIPS.

Results

Successful modeling

In this study, a second-order Bézier curve and an arc model were utilized to model the puncture needle. The positions of the modeled puncture needle's P2 points were compared with actual measurements. The results indicated that the error between the second-order Bézier curve model and the actual measured values was 0.15 cm, while the error for the arc model was 0.19 cm. Both modeling methods effectively support puncture needle modeling; however, the second-order Bézier curve model exhibited a smaller error and demonstrated higher accuracy.

Error analysis

Ten repeated measurements were conducted for the coordinates of the IP point and the TP point. The results showed that under the current level of measurement error, the coordinates of the IP point were (−0.40 cm ±0.02 cm, −4.45 cm ±0.02 cm), and the coordinates of the TP point were (−2.18 cm ±0.02 cm, −6.41 cm ±0.03 cm). Based on the Monte Carlo simulation to analyze the propagation effect of measurement errors, the optimal bending angle for this patient was determined to be 42.19° ±0.64° (95% CI 41.00–43.00°). The angle estimation exhibited high reproducibility, with a coefficient of variation (CV) of 2.90%. The minimum portal vein diameter of the 32 patients was 0.38 cm, and the permissible range of the error angle was ultimately calculated to be 3°.

Clinical effect evaluation

Among the 32 patients who underwent TIPS, the α values calculated based on the algorithm were compared with the α values actually measured during surgery (Table 1). Statistical analysis revealed that both the measured α values and the algorithm-calculated α values followed a normal distribution. The mean difference between the two was 1.06° ±1.82 (95% CI 0.41–1.72°), with a Cohen's d effect size of 0.14, indicating a small effect

Table 1 Target penetration point and bending angle

Patient	IP(x,y)	TP(x,y)	Intraoperative α/°	Calculated α/°
1	(−1.08, −6.76)	(−3.00, −10.39)	24.81	28.00
2	(−0.39, −5.51)	(−1.87, −8.84)	19.33	20.00
3	(−0.18, −4.62)	(−1.76, −6.74)	37.19	36.00
4	(−0.43, −5.81)	(−2.43, −7.60)	48.84	48.00
5	(0.29, −6.52)	(−2.79, −10.74)	32.51	36.00
6	(−0.29, −4.51)	(−1.68, −7.68)	25.63	24.00
7	(−0.24, −4.56)	(−1.32, −6.65)	23.30	28.00
8	(0.27, −5.79)	(−2.10, −8.72)	36.78	40.00
9	(−0.93, −4.82)	(−2.60, −7.39)	33.59	32.00
10	(−0.69, −3.46)	(−2.22, −6.56)	28.77	28.00
11	(−0.63, −3.99)	(−4.15, −6.75)	46.77	48.00
12	(−0.32, −6.35)	(−3.35, −10.50)	31.89	36.00
13	(−1.03, −5.48)	(−3.48, −7.70)	26.54	28.00
14	(−0.21, −4.85)	(−1.82, −9.13)	20.16	22.00
15	(−0.36, −5.59)	(−3.18, −9.64)	32.91	34.00
16	(−0.40, −4.47)	(−2.17, −6.40)	38.50	42.00
17	(−0.39, −5.38)	(−2.95, −8.50)	41.17	40.00
18	(−0.45, −5.16)	(−2.05, −7.08)	40.07	40.00
19	(−0.23, −4.16)	(−2.77, −7.50)	38.95	38.00
20	(−0.46, −4.42)	(−3.39, −7.34)	43.98	46.00
21	(−0.51, −3.92)	(−2.80, −6.80)	38.27	38.00
22	(−0.64, −4.46)	(−2.41, −6.87)	36.72	36.00
23	(−0.29, −5.24)	(−3.60, −10.21)	31.88	34.00
24	(−0.43, −4.93)	(−3.04, −7.24)	45.03	48
25	(−0.27, −5.15)	(−2.91, −8.44)	41.08	40
26	(−0.39, −5.48)	(−1.79, −8.82)	22.18	24
27	(−0.20, −3.23)	(−1.89, −6.00)	32.49	32
28	(−0.52, −5.64)	(−2.33, −7.98)	35.15	36
29	(−0.21, −5.21)	(−3.07, −9.25)	34.65	36
30	(−0.70, −4.73)	(−3.25, −8.23)	33.69	36
31	(−0.53, −5.48)	(−1.99, −7.24)	39.42	40
32	(−0.28, −5.42)	(−3.37, −10.41)	29.73	32

IP insertion point, *TP* target point, α bending angle of the penetration needle

size for the difference. Within the pre-defined clinically acceptable equivalence margin (± 3°), the two values demonstrated significant equivalence ($p < 0.001$). Additionally, detailed clinical statistical results for the 9 cases of initial puncture failure are provided in Table 2.

Discussion

The TIPS technique is distinguished by its minimal invasiveness and a reduced likelihood of adverse events. Nevertheless, it necessitates a proficient level of technical expertise, notably during the crucial stage of puncturing between the hepatic vein and the portal vein [11, 12]. Given the intricate anatomical configuration of the hepatic vasculature and notable interpatient variability, it is imperative to carefully adjust the bending angle of the puncture needle prior to the intervention. Improper choice of the puncture

Table 2 Statistical data of initial puncture failure cases in TIPS surgery

Patient	Number of punctures	Puncture time/min	Initial puncture α/°	Final puncture α/°	Calculated α/°
a	2	11.23	31.91	45.03	48
b	3	44.85	30.84	41.08	40
c	3	22.06	38.27	22.18	20
d	2	0.30	32.54	32.49	32
e	2	0.97	33.58	35.15	36
f	2	1.27	34.41	34.65	36
g	3	28.95	33.92	33.69	36
h	3	60.82	25.05	39.42	40
i	3	3.38	30.21	29.73	32

angle may result in recurrent punctures or puncture failure [13]. Moreover, the act of repeatedly bending the needle during the puncture procedure could lead to a decrease in support strength [14].

To address the aforementioned challenges, this study utilized preoperative contrast-enhanced CT imaging to determine the hepatic vein puncture IP point and portal vein puncture TP point. The puncture needle was modeled using Bézier curves to quantitatively calculate its bending angle, combined with Mimics software for three-dimensional path planning, aiming to reduce puncture attempts and surgical difficulty [15]. Compared with existing methods, our approach demonstrates several advantages: first, unlike conventional methods (such as Zhu et al.'s approach calculating the bending angle based on the relative position of target puncture points [10], or techniques shaping the puncture needle by measuring the relative positions of the IP and TP points [16]), our method incorporates not only the spatial relationship between the right hepatic vein and the target portal vein puncture point, but also integrates the anatomical relationship with the inferior vena cava. Furthermore, we validated whether the planned path conformed to the vascular spatial anatomy. Second, compared with methods calculating bending angles using three-dimensional path planning software [17], our approach eliminates the need for additional arterial catheterization and angiography [18], thereby significantly reducing radiation exposure and contrast agent dosage. This advantage is particularly valuable for cases where the portal vein is poorly visualized due to wedged hepatic venography—a common challenge when using existing three-dimensional path planning software.

This study retrospectively analyzed data from 32 patients who underwent TIPS procedures, including 2 cases with atypical hepatic vasculature, and compared the actual bending angles of the puncture needle during surgery with the bending angles calculated based on the algorithm. Statistical analysis revealed that the angles calculated by the algorithm demonstrated good equivalence with the actual angles required for successful puncture, providing strong evidence for the feasibility of the algorithm in clinical applications. Among the 2 cases with atypical hepatic vasculature, the errors between the actual bending angles during surgery and the algorithm-calculated angles were 1.09° and 2.31°, respectively, indicating that the algorithm maintains high accuracy even in complex anatomical structures. Although certain errors exist in the measurement of the IP point and TP point coordinates, Monte Carlo simulation analysis demonstrated that

these measurement errors had an impact of less than 1° on the optimal bending angle, which is within the clinically acceptable range. Additionally, the angle estimation in this study exhibited high reproducibility, with a CV of 2.90%, further validating the effectiveness and stability of the algorithm in clinical practice.

Nine cases of initial puncture failure during TIPS surgeries were analyzed. Among them, three cases of puncture failure were attributed to the improper selection of the bending angle of the puncture needle. This was mainly due to the insufficient preoperative evaluation of the anatomical structure of the hepatic blood vessels. Given the complex relationship between the portal vein and the hepatic veins, the puncture angle could not be precisely planned, resulting in the puncture path deviating from the target. The longest puncture time reached 44.85 min, which significantly increased the radiation exposure of both patients and medical staff. In addition, three cases of puncture failure were caused by the improper puncture direction, as the doctors inaccurately evaluated the spatial relationship between the hepatic veins and the portal vein during the operation. One case was due to the significantly enhanced hardness of the liver tissue caused by liver cirrhosis, which increased the puncture resistance. One case was caused by the cavernous transformation of the portal vein, leading to a remarkable increase in the difficulty of puncture, indicating the significant influence of anatomical factors on the complexity of the surgery. There was another case where puncture failure occurred due to the poor visualization of the portal vein. Although successful puncture was achieved after the placement of a positioning catheter, the operation time was prolonged. These findings highlight the importance of quantitatively calculating the bending angle of the puncture needle and conducting preoperative path planning.

Although this study is a retrospective one and has not been directly compared with traditional surgical methods, existing research has shown that constructing a three-dimensional model using Mimics software and estimating the bending angle of the puncture needle based on the spatial relationship [19], or designing a"body surface positioning guide plate"and a"puncture angle corrector"based on CT data for preoperative planning and intraoperative guidance can effectively reduce the incidence of perioperative complications, shorten the operation time, reduce the number of punctures, and improve the success rate of the surgery [20]. In this study, the bending angle of the puncture needle was optimized through an algorithm, and the potential of this approach in reducing the risk of puncture failure and improving surgical efficiency was preliminarily verified. Future research will design prospective clinical trials to systematically compare key indicators such as the fluoroscopy time and the surgical success rate of the two methods, so as to further validate the clinical advantages of this algorithm.

This study has certain limitations: (1) there may be measurement errors when measuring the IP point, TP point, and the bending angle α. In subsequent studies, these will be improved by using more precise measurement tools or methods. (2) Due to human physiological activities (such as respiratory movements and vascular pulsations), the puncture site may be displaced, which affects the puncture accuracy to a certain extent. In future research, patients will be guided to hold their breath during calm breathing through preoperative scans and during intraoperative puncture to reduce the impact of respiratory movements on puncture accuracy. (3) The morphological changes at the proximal end of the puncture needle during bending, as well as the minute compression

and deformation the needle experiences during the puncture process, were overlooked. In future research, the incorporation of physiological and mechanical factors will be undertaken to enhance the accuracy and practicality of the puncture needle model.

Conclusion

In conclusion, this study has devised an algorithm for determining the optimal bending angle of the puncture needle used in TIPS, along with a three-dimensional path planning method, aimed at guiding the implementation of TIPS procedures. Comparative analysis was conducted on patients who underwent successful TIPS procedures, demonstrating that this method is rational, effective, and holds potential for clinical application.

Methods

Mathematical modeling

First, mark the puncture needle tip of the RUPS100 puncture kit at specific points, as shown in Fig. 1. The starting point of the bend is designated as P0, the endpoint of the bend at the end of the gray catheter is P2, and the needle tip is labeled as P3. The angle between the tangent at the bending point and the tangent at the needle tip is defined as β, and the intersection of the two tangents is denoted as P1. The length of the bent portion of the gray catheter is L. The initial state of the puncture needle was measured for angle and length, yielding the following data: L = 5.5 cm, β = 20°, P0P1 = 2.4 cm, P1P2 = 3.0 cm, and P2P3 = 3.0 cm. A Cartesian coordinate system was established with point P0 as the origin (0, 0); the long axis of the puncture needle aligns with the y-axis, while the perpendicular direction represents the x-axis. Through geometric relationships, the coordinates of point P1 were calculated as (0, −2.4), P2 as (−1.03, −5.22), and P3 as (−2.06, −8.04). The following section introduces two methods for modeling the puncture needle: one is based on second-order Bézier curves, and the other utilizes arc modeling.

Second-order Bessel curve modeling

The bending section of the puncture needle from P0 to P2 can be approximated as a Bézier curve, as shown in Fig. 2a. The Bézier curve is a smooth curve developed by the French mathematician Pierre Bézier through mathematical methods and has been widely used. It is commonly applied in data fitting and graphic design. Given the

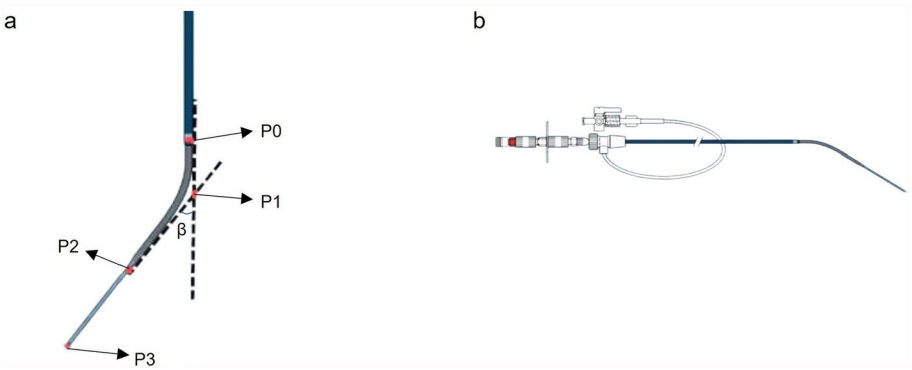

Fig. 1 The morphology of the puncture needle. The picture is sourced from the Internet. **a** Marking of the tip position of the puncture needle. **b** RUPS100 puncture kit

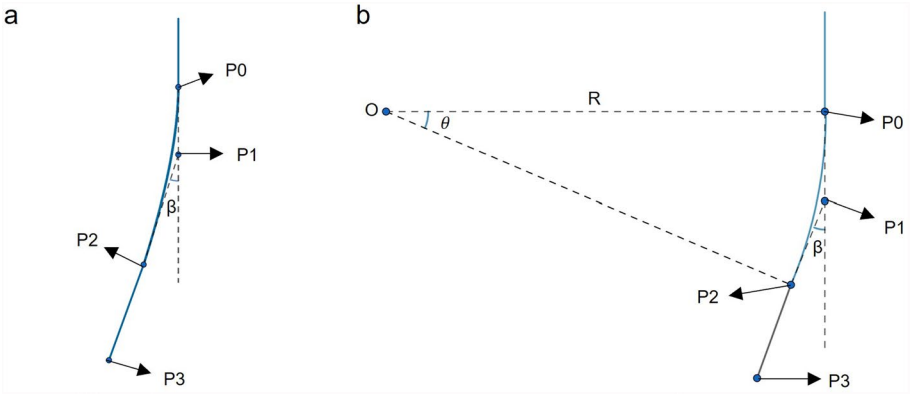

Fig. 2 Modeling of the puncture needle. **a** Modeling a puncture needle using Bézier curves. **b** Modeling a puncture needle with arc lines

coordinates of points P0 and P1, the angle β, and the length L of the catheter. On this basis, according to the equation of the line:

$$y = kx + b. \tag{1}$$

The linear equation between points P1 and P2 is determined by substituting the given data. Next, iterate through each point on the line, assuming the point as P2, and substitute it into the equation of a second-order Bézier curve:

$$B_{(t)} = (1-t)^2 P0 + 2(1-t)P1 + t^2 P2, t \in [0,1]. \tag{2}$$

Dividing the parameter t in the formula into 10 equal segments within the interval [0, 1], the coordinates of points on the Bézier curve B(t) are determined through piecewise computation. Using the curve integral formula:

$$L = \int_a^b \sqrt{x_{(t)}^2 + y_{(t)}^2 dt}, t \in [0,1]. \tag{3}$$

Bézier curve length is calculated in segments. When the sum of the lengths approaches 5.50 cm, the position of point P2 is determined. By substituting relevant data the coordinates of point P2 ultimately calculated to be (−1.08, −5.36).

Arc modeling

The bent portion of the puncture needle approximately forms an arc. The central angle of this arc is denoted as θ, with a radius of R, starting from point p0 to point p2, with an arc length of L. The tangents of the arc at its two endpoints intersect at point P1, forming an angle β, as illustrated in Fig. 2b. Establish the Cartesiancoordinate system as described above, where it is evident from geometric relationships that θ = β. The coordinates of point P2 can then be expressed as $(-R + R\cos\theta, -R\sin\theta)$. By substituting the data into the formula for arc length:

$$L = \frac{n\pi R}{180^0}. \tag{4}$$

It is computed that the coordinates of point P2 are (−0.95, −5.39).

Second-order Bessel curves and arcs

Error calculation of the P2 point coordinates of the actual puncture needle compared to the puncture needle modeling of second-order Bessel curves and arc modeling. The error calculation formula is as follows:

$$d = \sqrt{(x_a - x_b)^2 + \left(y_a - y_b\right)^2}, \tag{5}$$

where (x_a, y_a) represents the coordinates of the modeled puncture needle's P2 point, and (x_b, y_b) corresponds to the coordinates of the actual puncture needle's P2 point. By substituting relevant data for error calculation, it is concluded that the modeling error of the second-order Bézier curve is relatively small. Therefore, the Bézier curve is used for modeling and calculation of the puncture needle.

Calculation and validation

Puncture point selection

The portal venous phase CT images were imported into Mimics software, where a combination of thresholding and morphological operations was used to extract the hepatic and portal veins, enabling three-dimensional visualization. Based on the requirements of the TIPS clinical practice guidelines [21] and the spatial anatomical relationships between the hepatic and portal veins, interventional radiologists selected multiple puncture points. The method is as follows: three initial points (IP) are selected at a distance of 1–2 cm from the bifurcation of the inferior vena cava at the right hepatic vein. Similarly, three portal vein terminal points (TP) are selected at the bifurcation of the portal vein and 1.5 cm distally. For patients with atypical hepatic vasculature, the target puncture points were selected individually based on their vascular anatomical characteristics. Additionally, based on the doctor's experience, at an appropriate level, the four endpoints (anterior, posterior, left, and right) of the inferior vena cava are selected as the starting points (P0) for the bending of the puncture needle. Finally, three points are chosen from the aforementioned selections as the tentative points for IP, TP, and P0.

Construction of the puncture plane

Based on the selected IP, TP and P0 points, use the geometric modeling function of the Mimics software to establish the puncture plane. Taking the direction in which the puncture needle enters as the y-axis and the direction perpendicular to the puncture needle's entry direction as the x-axis, establish a Cartesian coordinate system. Use the second-order Bézier curve modeling in the coordinate system to draw the initial shape of the puncture needle, connect point P2 and point P3, and mark the positions of point IP and point TP, as shown in Fig. 3.

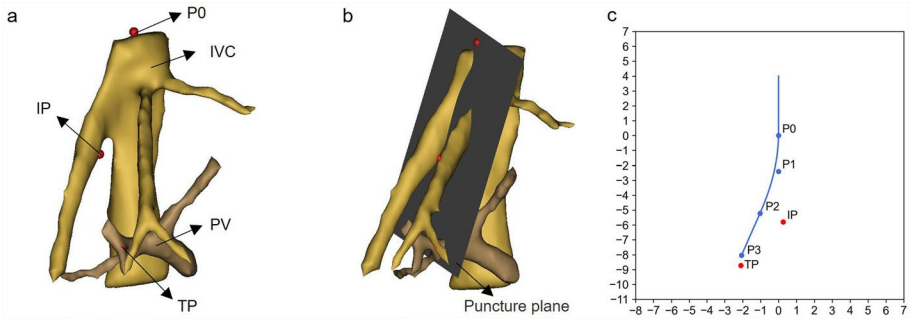

Fig. 3 Puncture needle and target puncture point. **a** Liver blood vessels and target puncture point, IVC inferior vena cava, PV portal vein. **b** Created puncture plane. **c** Position of the puncture needle curve modeled with a second-order Bézier curve in the established Cartesian coordinate system

Bending angle calculation

Firstly, determine whether the puncture needle in the initial state can puncture through point IP to point TP. If it cannot puncture, then subsequent optimization steps are required. (1) Uniformly select nine candidate bending points M on the curve from point P0 to point P2. Rotate the curve part from point M to point P3 around point M. The formula for rotation coordinates is as follows:

$$\begin{cases} x' = (x - rx) \times \cos\theta - \left(y - ry\right) \times \sin\theta + \gamma x \\ y' = (x - rx) \times \sin\theta + \left(y - ry\right) \times \cos\theta + ry \end{cases}, \theta \in \left[0^{\circ} \sim 40^{^{\circ}}\right], \tag{6}$$

where $\left(x, y\right)$ represents any point, (rx, ry) is the coordinates of the rotation center, and θ is the rotation angle. $\left(x', y'\right)$ denotes the new coordinates after rotation. Substitute the points on the curve MP2 and the straight line P2P3 into Formula 6 to obtain the rotated curve and straight line, and then curve of the bent puncture needle can be obtained. (2) To determine the optimal bending angle, the error between the slope of line $P2'P3'$ and the slope of line IPTP is calculated for each rotational angle. The formula for the slope error is as follows:

$$k_{(P2'P3')} - k_{(IPTP)} = \frac{y_3 - y_2}{x_3 - x_2} - \frac{y_T - y_I}{x_T - x_I}. \tag{7}$$

When the slope errors of both are minimized, the line $P2'P3'$ is approximately parallel to the line IPTP. (3) The coordinate difference between $P2\prime$ and IP is:

$$\begin{cases} \Delta x = X_{IP} - x_2' \\ \Delta y = Y_{IP} - y_2' \end{cases}. \tag{8}$$

After bending, the curve coordinates of the puncture needle move by $(+\Delta x, +\Delta y)$ so that point P2'coincides with point IP, and point TP lies on or near the line P2'P3', facilitates the puncture needle piercing from point IP to point TP, as shown in Fig. 4. This corresponds to the optimal bending angle $\alpha = \theta + \beta$

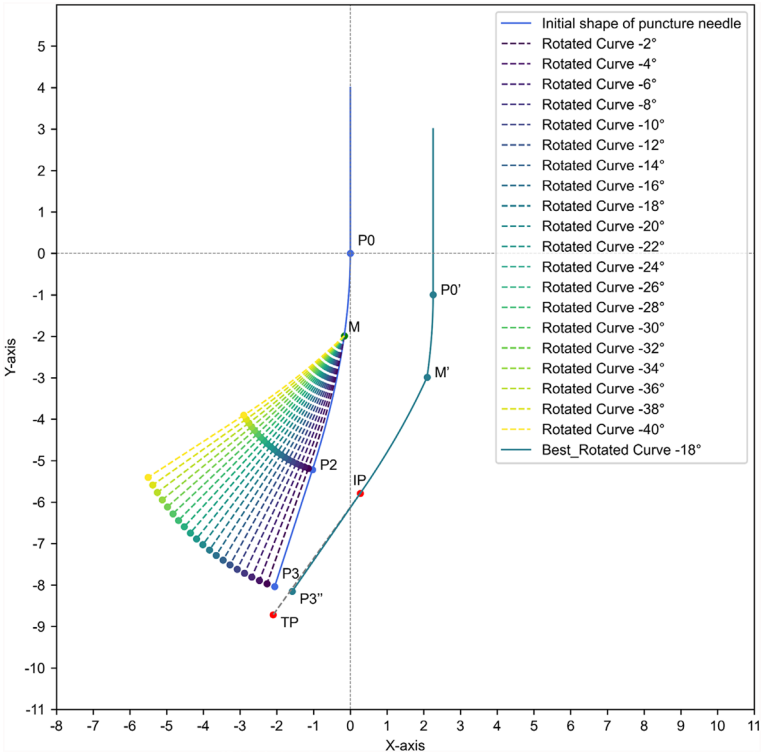

Fig. 4 Rotation of the puncture needle curve around point M. The blue curve represents the initial path of the puncture needle, while the purple, green, and other colors depict the trajectory of the needle after bending around point M. The green curve in the lower right corner represents the trajectory of the puncture needle after bending at the optimal angle and translating

Evaluation of outcomes

Select 10 points uniformly along the translated puncture needle curve and mark them in the puncture plane. These points should then be connected to form a curve, along with the IP and TP points, allowing for the completion of puncture path planning. The appropriateness of the puncture pathway is verified by assessing the position of the curve within the blood vessel. If the puncture pathway is deemed unsuitable, the M point is to be adjusted; should all M points be deemed unsuitable, a change in the puncture plane is warranted. The flowchart of the entire algorithm is illustrated in Fig. 5.

Clinical trial

Retrospective collection of preoperative enhanced CT images, intraoperative DSA images, and postoperative CT images was conducted for 32 patients who underwent TIPS surgery at this hospital between January 2023 and April 2025, including 9 cases with initial puncture failure. The locations of the preoperative CT images IP and TP points were determined based on the stent placement observed in the postoperative CT images, and the bending angle α of the puncture needle was measured from the DSA images during the procedure. The interventional radiologist selected an appropriate P0 point for each case, and the optimal bending angle α was calculated using the methods described above.

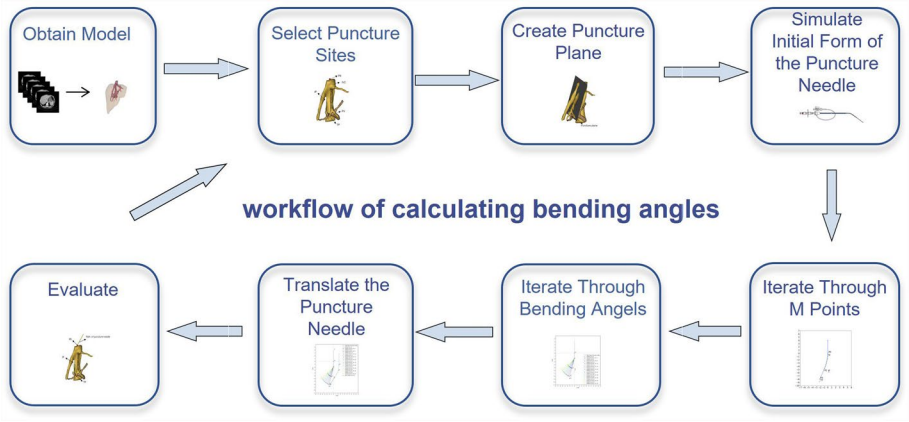

Fig. 5 Algorithm flowchart. This figure was created by Figdraw

Error calculation

To evaluate the impact of measurement errors on angle calculations, the coordinates of the puncture points (IP, TP) were measured 10 times by an interventional radiologist for a randomly selected patient. Based on these measurements, 1,000 samples were randomly generated using Monte Carlo simulation, and the angle distribution was calculated using the aforementioned algorithm. By analyzing the simulation results, the influence of measurement errors on angle calculations was quantified, thereby assessing the robustness of the algorithm. In addition, the diameter of the portal vein at the puncture plane was measured for 32 patients in this study. By iterating through the puncture needle bending angles in increments of 1°, the angle corresponding to the movement of point P3 to the minimum portal vein diameter was calculated and defined as the permissible range of error angles.

Statistical analysis

In this study, Python 3.10.9 was used for statistical analysis. For quantitative data, the mean ± standard deviation was used for description, and the Shapiro–Wilk test was performed to assess the normality of the data. An equivalence test was conducted to evaluate whether the measured bending angle and the calculated bending angle were equivalent within a clinically acceptable range.

Abbreviations

TIPS	Transjugular intrahepatic portosystemic shunt
CT	Computed tomography
IP	Initial points
TP	Terminal points
DSA	Digital subtraction angiography
CV	Coefficient of variation

Acknowledgements

Not applicable.

Author contributions

L.B proposed the key idea for the research. H.W.J participated in the study design and supervised the research. H.X.Y and G.J.C participated in data collection and analysis. L.B and Z.Y.Z were involved in the experimental design. The first draft was co-written by L.Q.M and H.X.H. All authors participated in the final approval.

Funding

Not applicable.

Availability of data and materials
Data sets supporting the findings of this study can be made available upon reasonable request to the corresponding author.

Declarations

Ethics approval and consent to participate
The study has been approved by the Ethics Committee of North Sichuan Medical College. Due to the retrospective nature of the research, informed consent is not required.

Consent for publication
Not applicable.

Competing interests
The authors declare no competing interests.

Received: 10 February 2025 Accepted: 13 May 2025
Published online: 27 May 2025

References

1. Lee HL, Lee SW. The role of transjugular intrahepatic portosystemic shunt in patients with portal hypertension: advantages and pitfalls. Clin Mol Hepatol. 2022;28:121–34.
2. Masek J, Fejfar T, Frankova S, Husova L, Krajina A, Renc O, et al. Transjugular intrahepatic portosystemic shunt in liver transplant recipients: outcomes in six adult patients. Vasc Endovascular Surg. 2023;57:373–8.
3. Nardelli S, Bellafante D, Ridola L, Faccioli J, Riggio O, Gioia S. Prevention of post-tips hepatic encephalopathy: the search of the ideal candidate. Metab Brain Dis. 2023;38:1729–36.
4. Wong F. Management of refractory ascites. Clin Mol Hepatol. 2023;29:16–32.
5. Mamone G, Milazzo M, Di Piazza A, Caruso S, Carollo V, Gentile G, et al. Transjugular intrahepatic portosystemic shunt (TIPS) complications: what diagnostic radiologists should know. Abdom Radiol N Y. 2022;47:4254–70.
6. Vizzutti F, Schepis F, Arena U, Fanelli F, Gitto S, Aspite S, et al. Transjugular intrahepatic portosystemic shunt (TIPS): current indications and strategies to improve the outcomes. Intern Emerg Med. 2020;15:37–48.
7. Richards L, Dalla S, Fitzgerald S, Walter C, Ash R, Miller K, et al. Utilizing 3D printing to assist pre-procedure planning of transjugular intrahepatic portosystemic shunt (TIPS) procedures: a pilot study. 3D Print Med. 2023;9:10.
8. Rêgo HMC, Medronha EF, Junior EZ, Tovo CV, de Mattos AA. Transjugular intrahepatic portosystemic shunt with transhepatic portal vein puncture guided by ultrasound: a technical alternative. Eur J Gastroenterol Hepatol. 2022;34:112–6.
9. Rahimi RS, Rockey DC. Complications of cirrhosis. Curr Opin Gastroenterol. 2012;28:223–9.
10. Zhu X, Ran Z, Li W, Wang W, Zhu K, Huang W, et al. Method for calculating the bending angle of puncture needle in preoperative planning for transjugular intrahepatic portal systemic shunt (TIPS). Comput Math Methods Med. 2018;2018:4534579.
11. Lucatelli P, Krajina A, Loffroy R, Miraglia R, Pieper CC, Franchi-Abella S, et al. CIRSE standards of practice on transjugular intrahepatic portosystemic shunts. Cardiovasc Intervent Radiol. 2024;47:1710–26.
12. Qin J, Tang S, Jiang M, He Q, Chen H, Yao X, et al. Contrast enhanced computed tomography and reconstruction of hepatic vascular system for transjugular intrahepatic portal systemic shunt puncture path planning. World J Gastroenterol. 2015;21:9623–9.
13. Xu T, Hou P, Su Y, Wei L, Wu F. Application of 3D image fusion technology in transjugular intrahepatic portosystemic shunt. Chin J Minim Invasive Surg. 2023;23:336–40.
14. Liu Y, Zhang K, Liu J, Guo Z, Dang R. Application of 3D printing technology to transjugular intrahepatic portosystemic shunt in patients with cirrhotic portal hypertension complicated with gastrointestinal bleeding. Chin Med Equip J. 2022;43:54–8.
15. Zhang Y, Liu F. Precision technique and rational shunt in transjugular intrahepatic portosystemic shunt. J Pract Hepatol. 2022;25:5–8.
16. Huang J, Zhang Q, Gao X, Chen H, Zheng J. Application of CT image-guided pre-puncture shaping technique in transjugular intrahepatic portosystemic shunt. J Interv Radiol. 2023;32:63–6.
17. Tsauo J, Luo X, Ye L, Li X. Three-dimensional path planning software-assisted transjugular intrahepatic portosystemic shunt: a technical modification. Cardiovasc Intervent Radiol. 2015;38:742–6.
18. Luo X, Wang X, Yu J, Zhu Y, Xi X, Ma H, et al. Transjugular intrahepatic portosystemic shunt creation: three-dimensional roadmap versus CO2 wedged hepatic venography. Eur Radiol. 2018;28:3215–20.
19. Sun M, Xu X, Pan L, Meng Q, Feng Y, Zhang G. Application research of three-dimensional models in transjugular intrahepatic portosystemic shunt. Chin J Exp Surg. 2024;41:2215–8.
20. Zhang K, Liu J, Liu Y, An Z, Li X, Meng Y. Observation of clinical effectiveness of computer-generated 3D models using CT thin-slice scanning data to guide transjugular intrahepatic portosystemic shunt for the treatment of cirrhotic portal hypertension with gastrointestinal bleeding. Clin J Med Off. 2023;51:655–6.
21. Chinese College of Interventionalists. CCI clinical practice guidelines: management of TIPS for portal hypertension (2019 edition). Chin J Hepatol. 2019;27:582–93.

Publisher's Note